THE ASTROPHYSICAL JOURNAL, 445:98–107, 1995 May 20

CHEMICAL EVOLUTION OF IRREGULAR AND BLUE COMPACT GALAXIES

LETICIA CARIGI
Centro de Investigaciones de Astronomía, Apdo. Postal 264, Mérida 5101-A, Venezuela; carigi@cida.ve
AND
PEDRO COLÍN, MANUEL PEIMBERT, AND ANTONIO SARMIENTO
Instituto de Astronomía, UNAM, Apdo. Postal 70-264, 04510 México, D.F., Mexico;
colin@astroscu.unam.mx, peimbert@astroscu.unam.mx, ansar@astroscu.unam.mx
Received 1994 September 9; accepted 1994 December 1

ABSTRACT

We discuss the chemical evolution of metal-poor galaxies and conclude that their oxygen deficiency is not due to the production of black holes by massive stars or a varying slope of the initial mass function, IMF, at the high-mass end. A varying IMF at the low-mass end alone or in combination with (*a*) an outflow of oxygen-rich material, (*b*) an outflow of well-mixed material, and (*c*) the presence of dark matter that does not participate in the chemical evolution process is needed to explain their oxygen deficiency. Outflow of material rich in O helps to account for the large $\Delta Y/\Delta O$ values derived from these objects, but it works against explaining the (Z − C − O)/O and C/O values.

Subject headings: cooling flows — galaxies: abundances — galaxies: compact — galaxies: evolution — galaxies: ISM — stars: luminosity function, mass function

1. INTRODUCTION

By studying the O-μ diagram for irregular and blue compact galaxies, where O is the oxygen abundance mass fraction and μ is the gas mass fraction, it is found that for a given μ value, the O value is smaller than the one predicted by the closed-box model of chemical evolution with an IMF independent of Z. In a review of this problem by Peimbert, Colín, & Sarmiento (1994a), it is argued that the small O values are not due to (*a*) errors in the O determination, (*b*) inflow, (*c*) variations of the slope of the IMF at the high-mass end, or (*d*) the production of black holes by massive stars. Alternatively, these authors argue that the observed values in the O-μ diagram could be due to (*a*) outflow, (*b*) variations of the IMF at the low-mass end, (*c*) the presence of dark matter that does not participate in the chemical evolution process, or (*d*) errors in the determination of the total mass of the galaxies, M_T. We shall make quantitative estimates of some of these effects based on a comparison of chemical evolution models of galaxies with observations. In addition to the O and μ values, we have three additional observational restrictions that can be used to constrain the models: the enhancement in the helium to oxygen mass ratio, $\Delta Y/\Delta O$, the carbon to oxygen mass ratio, C/O, and the heavy elements minus carbon and oxygen to oxygen mass ratio (Z − C − O)/O.

In § 2 we describe the chemical evolution models of galaxies; in § 3 we select 10 objects from the best observed ones and obtain representative values for O, μ, $\Delta Y/\Delta O$, C/O, and (Z − C − O)/O, values that should be reproduced by the models. In § 4 we compare the observational constraints with the predictions made by closed-box models with a varying mass threshold, m_{bh} (hereafter *m* denotes mass in solar mass units), for the end of the evolution of massive stars as black holes (i.e., without enriching the interstellar medium, ISM, with the heavy elements that are ejected when the massive stars explode in supernovae events, SNs); these models are computed without the assumption of the instant recycling approximation, IRA (i.e., taking into account the time delay involved in the ISM enrichment), for two families of IMFs, and variable ages. In § 5 we present two types of galactic outflow models and compare them with the observations. Finally, the discussion and conclusions are presented in § 6.

2. CHEMICAL EVOLUTION MODEL

2.1. *Main Features*

Our chemical evolution model for irregular galaxies takes into account the dependence of the element yields with the metallicity of the parent galaxy; it is essentially the model presented by Carigi (1994) for the solar neighborhood with the following modifications: a well-mixed or an O-rich galactic wind is added, the infall is excluded, and the initial gas abundances are chosen as pregalactic ($X_p = 0.77$, $Y_p = 0.23$, and $Z_p = 0$). Our model considers ages of $t_g = 0.1$, 1, and 10 Gyr; that is, models are differentiated from each other in the sense that they reproduce the representative μ and O values at different times: 0.1, 1, and 10 Gyr. Prantzos, Vangioni-Flam, & Chauveau (1994) have also presented chemical evolution models of the Galaxy taking into account the effect of metallicity dependent yields.

The model by Carigi (1994) is an open one in which the yields, the lifetimes of stars, the masses of the remnant stars, and the masses of SN progenitors all depend on the metallicity of the progenitor cloud. The IRA is not used, and the evolution of H, ^{4}He, ^{12}C, ^{16}O, ^{56}Fe, and Z is modeled in detail; in particular, the He content does not increase linearly with metallicity. The star formation rate, ψ, is taken proportional to the gas mass: $\psi = \nu M_{gas}$. The stellar yields are nonlinearly interpolated from the set of metallicities presented by Maeder (1992), a procedure based on the results by Maeder (1991). Prantzos et al. (1994) also point out that a nonlinear interpolation for the yields improves the agreement of model predictions with observations in the Galaxy. The main-sequence lifetimes have been obtained from Schaller et al. (1992). The stars are divided into two mass intervals: (*a*) low-mass stars (LMSs), which are those with initial masses, m_i, in the 0.8 <

$m_i < 7.5$ range; and (*b*) high-mass stars (HMSs), those with initial masses in the $7.5 \leq m_i < 120$ interval. For LMSs, the C, O, and Z yields are taken from Renzini & Voli (1981) ($Z = 0.004$ and 0.02, $\alpha = 1.5$, $\eta = 1/3$), and the He yield and remnant masses from Maeder (1992, including stellar winds). For HMSs, all yields and remnant masses are taken from Maeder (1992, high–mass-loss rate). Three types of SNs are taken into account: Ia, Ib, and II. For SN Ib's, two possible progenitors are considered: Wolf-Rayet stars and binary systems; for this type of SNs, the Fe mass enrichment is 0.15 $M_\odot$, while for SN II's, it is taken as 0.075 $M_\odot$ (Nomoto, Shigeyama, & Tsujimoto, 1990).

2.2. *Stellar Models*

Since the yields calculated by Maeder (1992, 1993) are extensively used in what follows, we briefly describe the main features of the models by Maeder and collaborators; these are as follows:

Stars with m_i from 0.1 to 0.8 do not contribute to the interstellar gas enrichment and take gas only from the ISM when they are formed; their main-sequence lifetimes are greater than the age of the parent galaxy.

Stars with initial masses in the interval $0.8 \leq m_i < 1.85$ burn He in degenerate cores and end their lives as C-O white dwarfs. These stars enrich the ISM mainly with He, C, and N via stellar winds and planetary nebulae events; their main-sequence lifetimes vary from 1 to 25 Gyr depending on initial mass and metallicity.

Stars in the interval $1.85 \leq m_i < 7.5$ burn He in nondegenerate cores and when going through the asymptotic giant branch, enrich the ISM with He, C, and N via stellar winds until their existence ends in a C-O degenerate core after the ejection of a planetary nebula; their main-sequence lifetimes range from 0.03 to 1 Gyr; these stars, if in binary systems, may produce SN I's and contribute to the Fe enrichment, mainly.

Stars in the range $7.5 \leq m_i < m_{\rm wr}$ (lower limit mass for the formation of a Wolf-Rayet star) burn elements heavier than He and mainly eject He, C, N, and O via SN II's; their main-sequence lifetimes vary slightly with the initial chemical content and go from 0.003 to 0.03 Gyr. Appropriate values for $m_{\rm wr}$ are 25 for a solar metallicity, or 75 for 1/20 of the solar metallicity.

Stars with initial masses greater than $m_{\rm wr}$ and low metallicity contribute to the ISM enrichment with He, C, and O via SN Ib's and leave a massive remnant; for stars in the same mass range and high metallicities, the strong contribution to He and C, mainly, is via stellar winds and therefore, the remnants are less massive. Their lifetimes are less than 0.006 Gyr.

2.3. *Initial Mass Functions*

We have considered two initial mass functions: the first one is an extension of the IMF for the solar neighborhood derived by Kroupa, Tout, & Gilmore (1993) to lower masses in order to take into account substellar objects (hereafter KTG IMF), and the second one is the Salpeter (1955) IMF (hereafter S IMF). Both IMFs are normalized to one; that is,

$$\int_{m_l}^{m_u} m\xi(m)dm = 1 \ . \tag{2.1}$$

The lower and upper limits of the IMFs are considered to be 0.01 and 120, respectively.

The KTG IMF is given by

$$\xi(m) = \begin{cases} 0.510m^{-1.3} & \text{if } 0.01 \leq m < 0.5 \ , \\ 0.273m^{-2.2} & \text{if } 0.5 \leq m < 1.0 \ , \\ 0.273m^{-2.7} & \text{if } 1.0 \leq m < 120 \ , \end{cases} \tag{2.2}$$

where $\xi(m)dm$ is the number of stars in the mass interval from m to $m + dm$. For masses in the range $0.08 \leq m < 0.5$, KTG find that the exponent for the 95% confidence interval varies from -0.70 to -1.85 and the center is given by -1.3. The KTG IMF has the same slope for $m \geq 1$ as the Scalo (1986) IMF, i.e., the two IMFs have a different slope only for the $m < 1$ values. Though it has been ruled out by observations of the solar vicinity a while ago (Scalo 1986), the Salpeter IMF with a -2.35 value for the slope from $m = 0.01$ to 120 will be considered for comparison.

3. OBSERVATIONAL CONSTRAINTS

We will generate a series of models with the aim of fitting μ, O, $\Delta Y/\Delta$O, C/O, and $(Z - \mathrm{C} - \mathrm{O})$/O for a "typical" irregular galaxy. Thus, for any given galaxy, we need to know the values for these five constraints; however, it is not possible to derive $\Delta Y/\Delta$O for a single galaxy, and a determination using only a pair of galaxies would have a very poor quality; therefore, we will derive this value using the average ratio from a group of well-observed galaxies. The other four constraints will be obtained from average or representative values of the galaxies in this well-observed group.

3.1. M_T, μ, *and* O

In Table 1 we present a group of 10 galaxies with well-determined μ, O, and Y values. The data come from the following sources: (*a*) the Y values are taken from Lequeux et al. (1979), Pagel (1987), Torres-Peimbert, Peimbert, & Fierro (1989), Skillman (1991), Pagel et al. (1992, hereafter PSTE), Skillman & Kennicutt (1993), and Skillman et al. (1994); (*b*) the Z values are derived from the observed N(O)/N(H) values under the assumption that O constitutes 54% of the total Z value (see below); the N(O)/N(H) ratios are taken from Peimbert & Torres-Peimbert (1976), Dufour, Shields, & Talbot (1981), Kunth & Sargent (1983), Vigroux, Stasinska, & Comte (1987), Skillman, Kennicutt, & Hodge (1989), Garnett (1990), Schmidt & Boller (1993), Skillman & Kennicutt (1993), and Skillman et al. (1994); (*c*) the gaseous mass, $M_{\rm gas}$, the total mass, M_T, and their ratio, μ, are taken from Lequeux et al. (1979), and Staveley-Smith, Davies, & Kinman (1992). The colons after the μ values in the first two lines of Table 1 indicate that the M_T values are very uncertain for these two galaxies. The values of the total mass shown in Table 1 were obtained dynamically; therefore, they include any possible dark matter material, either baryonic or nonbaryonic. Our models assume that M_T is due only to the gaseous component, stars, substellar objects, and stellar remnants. The outflow models start with a higher total mass and reach the M_T value at the end of the evolution of each model. The last line in Table 1 contains the average values of the data in the previous rows. Since the average abundance values are calculated linearly, the relevance of the O-poor objects is much less than when the average values are calculated using the logarithms of the corresponding data. The representative value for $\Delta Y/\Delta$O is determined by the whole set of observations, and the role of the first two galaxies in our sample is mainly to help determine the value for the primordial He.

TABLE 1

PROPERTIES OF SELECTED GALAXIES

Galaxy	$\log (M_T/M_\odot)$	$\log (M_{gas}/M_\odot)$	$\log \mu$	Y	10^3O	10^3Z
I Zw 18	8.26	8.16	−0.1:	0.230	0.200	0.370
UCG 4483	7.94	7.84	−0.1:	0.239	0.403	0.746
Mrk 600	8.85	8.67	−0.18	0.240	1.241	2.297
SMC	9.18	8.80	−0.38	0.237	1.431	2.647
II Zw 40	8.87	8.40	−0.47	0.251	1.686	3.122
IC 10	9.73	9.11	−0.62	0.240	1.751	3.242
NGC 6822	9.23	8.28	−0.95	0.246	2.085	3.861
II Zw 70	9.11	8.58	−0.53	0.250	2.074	3.841
LMC	9.78	8.85	−0.93	0.250	2.608	4.829
NGC 4449	10.60	9.78	−0.82	0.251	2.856	5.288
Average[a]	9.15	8.65	−0.51	0.243	1.633	3.023

[a] Linear regressions: $Y = (0.232 \pm 0.004) + (7.10 \pm 1.62) \times \mathrm{O}$, $Y = (0.232 \pm 0.004) + (3.83 \pm 0.87) \times Z$.

The adopted values in this paper are $\log \mu = -0.53$, and $\log (M_T/M_\odot) = 9.12$. These values are slightly different from the average values presented in Table 1; nevertheless, a discussion on the effect produced by varying μ is given in §§ 4 and 6. The O values in Table 1 were derived by (*a*) adopting a uniform electron temperature over the observed H II region and (*b*) neglecting the fraction of O atoms tied up in dust grains.

From observations of H II regions in the solar neighborhood, it has been found that temperature variations along the line of sight increase the O/H ratio by about 0.3 dex (e.g., Peimbert, Torres-Peimbert, & Ruiz 1992; Peimbert, Storey, & Torres-Peimbert 1993a; Peimbert, Torres-Peimbert, & Dufour 1993b). From the study of a set of metal-poor H II galaxies, Campbell (1988) finds that the O/H ratios based on temperatures derived from the [O III] 4363/5007 ratio should be increased by factors in the 0.03–0.3 dex range, while from a similar set of objects, McGaugh (1991) finds that the O/H ratios should be increased by about 0.2 dex due to temperature variations along the line of sight. These temperature variations could be due to (*a*) the deposition of mechanical energy inside H II regions by stellar winds and SN explosions (e.g., Peimbert, Sarmiento, & Fierro 1991, and references therein), and (*b*) the presence of chemical abundance inhomogeneities. From this discussion and based mainly on the results by McGaugh (1991), Campbell (1988), and González-Delgado et al. (1994), we shall assume that the gaseous O/H ratio should be increased by 0.16 dex due to the temperature structure inside H II regions.

Dufour et al. (1995) have found that the ratio Si/O in irregular galaxies is from 1.5 to 3 times smaller than the solar value, indicating that an important fraction of the Si atoms is in the form of dust grains; this result implies that about 10% of the O atoms are trapped by Si, Mg, and Fe in dust grains. Consequently, the O abundance should be increased by 0.04 dex. These two corrections increase the O average value in Table 1 from 1.63×10^{-3} to 2.58×10^{-3}.

3.2. $\Delta Y/\Delta \mathrm{O}$

From a linear regression of the sample, it is found that $\Delta Y/\Delta \mathrm{O} = 7.10 \pm 1.62$. ΔO should be increased by 0.2 dex to take into account the temperature structure of the H II regions and the fraction of O embedded in dust; alternatively, ΔY is not affected by these two effects since the temperature structure diminishes the Y determinations but does not affect ΔY up to a very good approximation, and no He is expected to be in dust grains. Hence, we obtain for our sample that $\Delta Y/\Delta \mathrm{O} = 4.48 \pm 1.02$, and in the following we shall adopt $\log (\Delta Y/\Delta \mathrm{O}) = 0.65 \pm 0.11$ as the representative value to be fitted by our models.

We shall compare our $\Delta Y/\Delta \mathrm{O}$ determinations with those derived by other authors; in particular with PSTE, one of the most important data sets found in the literature. From these data it is found that $\Delta Y/\Delta \mathrm{O} = 10.2 \pm 3.5$, and combining them with the sample by Isotov, Thuan, & Lipovetsky (1994), it is found that $\Delta Y/\Delta \mathrm{O} = 9.7 \pm 2.8$. These values have been derived under the assumption of a uniform temperature inside the H II regions and without considering the amount of O embedded in dust grains, therefore in good agreement with the values derived from our sample.

From a comparison of Y_p with the O and Y abundances of the solar vicinity, Peimbert, Sarmiento, & Colín (1994b) have determined a value of $\Delta Y/\Delta \mathrm{O} = 5.22 \pm 1.1$, which is in excellent agreement with the value adopted by us for irregular galaxies.

3.3. C/O

The C/O ratio varies with O from a low value of about −1.1 dex for O-poor objects, to a high value of about −0.3 dex for the solar vicinity (Garnett et al. 1995; Peimbert 1993 and references therein). For the C/O constraint we shall consider well-observed objects with O values similar to those of our "typical" irregular galaxy; these are 30 Doradus in the LMC and NGC 2363 in NGC 2366. For 30 Doradus and NGC 2363, Garnett et al. obtain -0.60 ± 0.26 dex and -0.75 ± 0.15 dex, respectively, while Peimbert, Peña, & Torres-Peimbert (1986) obtain -0.65 ± 0.15 dex for NGC 2363. These results are not affected by the temperature structure since the lines used to derive the C and O abundances have similar excitation energies, and to a very good approximation the temperature structure cancels out. These three determinations correspond to the gaseous component and do not include the O trapped in dust grains. From these determinations and assuming that the fraction of O trapped in dust grains amounts to 0.04 dex, we shall adopt for the C/O ratio the value of -0.70 ± 0.15 dex.

We are assuming that the fraction of C embedded in dust grains is negligible. For the MNR/Draine-Lee grains (Mathis, Rumpl, & Nordsieck 1977; Draine & Lee 1984), made by a combination of silicate and graphite grains, the strengths of the 9.7 μm and 18 μm absorption features imply that practically all the Si atoms are in the Si—O stretch and consequently, that the amount of SiC is negligible (J. S. Mathis 1994, private communication). On the other hand, the 2175 Å bump, narrower in the H II regions than in the general ISM, is probably due to the removal of dust coatings by the higher radiation field and higher grain temperatures (Mathis 1994), and the high C/H values in the Orion Nebula and M17 (Peimbert et al. 1992; Peimbert 1993) also indicate that not much C is trapped by dust inside H II regions. In any case, a change in the adopted C/O constraint by 0.1 dex does not modify considerably our main conclusions (see Figs. 2 and 5).

3.4. $(Z - C - O)/O$

To determine the $(Z - C - O)/O$ value, we shall consider again the best observed irregular galaxies with O values similar to those of our "typical" irregular galaxy; these objects are 30 Doradus and NGC 2363. For 30 Doradus we shall take the C/O ratio from Garnett et al. (1995) and the N, O, Ne, S, and Ar values presented in Torres-Peimbert et al. (1989), increasing the O value by 0.04 dex to include the O trapped in dust grains. We shall assume that the mass ratio of all the other unobserved heavy elements to O is the same as in the Sun: 36% (Grevesse & Anders 1989; Grevesse et al. 1990; Biémont et al. 1991; Holweger et al. 1991; and Hannaford et al. 1992). From these values we obtain $(Z - C - O)/O = 0.645$ and $O/Z = 0.534$ for 30 Doradus. For NGC 2363 we shall take an average of the C/O ratios by Garnett et al. (1995) and Peimbert et al. (1986), while for N, O, Ne, S, and Ar we shall take the values from Peimbert et al. With the same assumptions as those adopted for 30 Doradus, we obtain that $(Z - C - O)/O = 0.660$ and $O/Z = 0.543$; these values can be compared to the solar ones that are 0.726 and 0.488, respectively; the differences are due to the smaller C/O and N/O values present in the irregular galaxies relative to the solar ones. From 30 Doradus and NGC 2363 we have adopted the value $\log [(Z - C - O)/O] = -0.18 \pm 0.06$.

4. CLOSED BOX MODELS

We have computed a series of closed box models—with and without the contribution of SN I's, for various IMFs, ages, and CO-core masses at the end of the C-burning phase, m_{CO}—in order to fit the adopted $\log \mu$ value of our sample and two possible values of O: 1.62×10^{-3}, and 2.58×10^{-3}. The variation of the CO core mass was used in order to study the suggestion by Maeder (1992, 1993), in the sense that black holes could play an important role in the chemical evolution of metal-poor galaxies; the models assumed that the entire star becomes a black hole if the mass of the CO-core is larger than m_{CO}.

In Figures 1, 2, and 3, a dot represents a model with an age of 10 Gyr, the KTG IMF, and $m_{CO} = 60$ (that is, without the presence of black holes), that fits the adopted values: $\log \mu = -0.53$ and $O = 2.58 \times 10^{-3}$. This model considers the contributions of SN I's of binary origin under the assumption that 5.7% and 2.4% of the binary systems become SN Ia's and Ib's, respectively; these are the fractions needed to adjust the current SN rates in the solar vicinity (see Carigi 1994). The SN I contributions to O and Z are only 2.3% and 10.1%, respectively; moreover, the SN I rates of irregular galaxies are not well known. For the 0.1 and 1 Gyr series of models, the contributions of SN I's to the chemical evolution of galaxies are completely negligible. Based on the previous discussion, the SN I's have not been taken into account for all the other models in this paper.

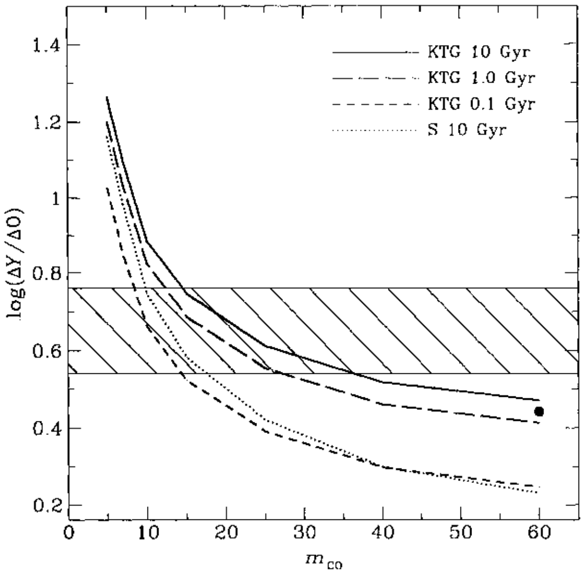

FIG. 1.—$\Delta Y/\Delta O$ vs. m_{CO} predicted by the closed models. The m_{CO} values that correspond to a given initial mass m (or to a given m_{bh}), are from Maeder (1992). The region allowed by observations is shown by a shaded band. The point represents a model with a KTG IMF, a galactic timescale of 10 Gyr, and including SN I's of binary origin.

In Figures 1, 2, and 3, we also present three series of models for the KTG IMF with different ages and one series of models for the S IMF with 10 Gyr. In Figure 3, the KTG curves for the 1 and 10 Gyr series are almost identical because the contributions by stars in the $0.9 < m_i < 1.85$ range to the $(Z - C - O/O)$ ratio are almost negligible. In Figures 1 and 2 the increase of $\Delta Y/\Delta O$ and C/O with t_g is due to the C and He enrichment of the ISM by LMS. The differences presented in Figures 1, 2, and 3 between the KTG 10 Gyr and the S series are mainly due to the larger number of stars in the $0.9 < m_i < 7.5$ interval in the KTG IMF compared to that in the S IMF.

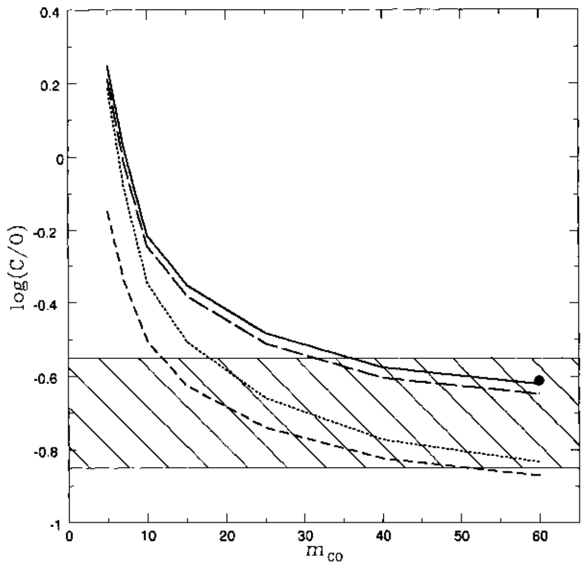

FIG. 2.—C/O vs. m_{CO} predicted by the closed models. The shaded band and the point have the same meaning as in Fig. 1, i.e., the region allowed by observations and the prediction when SN I's are included; different lines follow also the convention of Fig. 1.

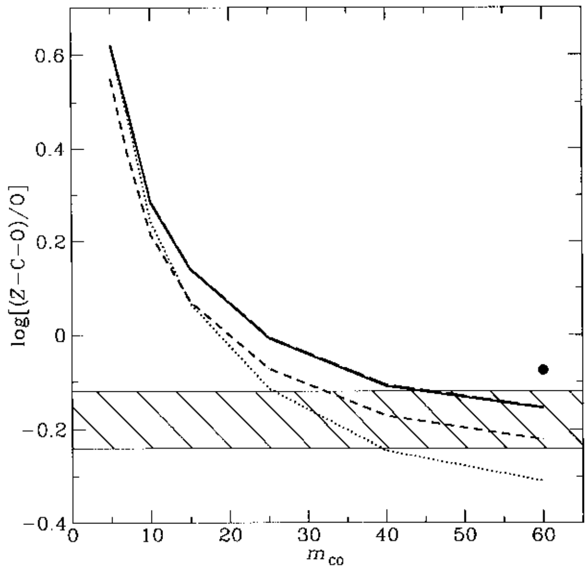

FIG. 3.—(Z − C − O)/O vs. m_{CO} predicted by the closed models. Regions, symbols, and notation have the same meaning as in the two previous figures.

Table 2 summarizes the results obtained by eight models with an age of 10 Gyr, a KTG IMF, and an initial mass gas of $1.33 \times 10^9\ M_\odot$. Seven of these models fit log $\mu = -0.53$ and $O = 2.58 \times 10^{-3}$ (see Table 1), while the eighth model fits the adopted log μ value and $O = 1.62 \times 10^{-3}$; the changes in the element ratios between the first and last rows in Table 2 are due to the dependence of the element yields on the initial Z. The first column shows m_{CO} values (related to m_{bh}) according to Maeder 1992). The two values present in the second column indicate the lowest stellar mass for the formation of a black hole when $Z = 0.001$, and to the same limit when each one of the models reaches its maximum metallicity. The third column shows the factor, r, by which the number of stars that contribute to the ISM enrichment has to be reduced in order to fit the adopted log μ and O values. The remaining columns give the values of the He, C, and Z abundances by mass, and some combinations of them.

In Table 3 we present the mass budget of the ISM from the different processes considered in four models with $m_{CO} = 60$ (i.e., no black holes present) and the KTG IMF. The columns are as follows: column (1), age of the model; column (2), chemical species; column (3), mass lost by star formation (SF); column (4), mass ejected by low-mass stars (LMS); column (5), mass ejected by the winds of high-mass stars (HMS_W); column (6), mass ejected by SN explosions (HMS_{SN}); and column (7), the ISM abundance by mass. In the contributions by the different stellar ejecta, both the material already present and the material synthesized within the stars are included.

From Table 2 and Figures 1, 2, and 3, it follows that there is not a unique m_{CO} value that fits the three observational restrictions for the 10 Gyr models. There are two extreme solutions that can be adopted: (*a*) we can fit the $\Delta Y/\Delta O$ value with $m_{CO} = 16.4$ that corresponds to an $r = 1.97$ but without satisfying the C/O and (Z − C − O)/O restrictions, or (*b*) we can fit C/O and (Z − C − O)/O with $m_{CO} = 60$ and $r = 3.39$ but without satisfying the $\Delta Y/\Delta O$ restriction. Note that the S IMF series and the KTG IMF 0.1 and 1 Gyr series predict even smaller $\Delta Y/\Delta O$ values than the KTG 10 Gyr series. Since star formation in the LMC and the SMC has been going on for about 10 Gyr, we consider the 10 Gyr series more adequate.

Carigi (1994) and Peimbert et al. (1994a, b) have found that the production of black holes by massive stars does not play an important role in the chemical evolution of the ISM in the solar vicinity. This result, combined with the C/O and (Z − C − O)/O constraints, has led us to consider that possibility (*b*) in the previous paragraph is more likely. The SN I contributions increase the predicted (Z − C − O)/O and C/O ratios by about 20% and 2%, respectively, making the presence of black holes more unlikely (see Figs. 2 and 3).

To reduce the O production, we have to adopt an IMF with a smaller fraction of massive stars to all the other stars. This can be done by either steepening the slope of the high-mass end of the IMF, or by increasing the amount of objects in the $0.01 < m < 1$ interval relative to those in the $1 < m < 120$ interval.

There are four arguments against changes in the slope at the high-mass end of the IMF with metallicity: (*a*) the study of the ionization degree of many extragalactic H II regions in irregular and blue compact galaxies with different O content (McGaugh 1991); (*b*) the observed continuum in the 1100–7500 Å range of starburst regions with different O content in M101 (Rosa & Benvenuti 1994); (*c*) direct determinations of the high-mass end slope in the SMC and the LMC (Massey et al. 1989a, b; Parker et al. 1992; Parker & Garmany 1993); and (*d*) since a more negative slope at the high-mass end of the IMF would also increase the predicted (Z − C − O)/O values, producing a conflict with the observations.

On the other hand, observational evidence and arguments in favor of a change at the low-mass end of the IMF, in the sense that the lower the metallicity, the larger the amount of small-mass stars, have been presented previously (Peimbert & Serrano 1982; Gusten & Mezger 1983; Larson 1986; Richer et al. 1991).

In what follows we will consider that the r values higher than 1 come from varying the IMF at its low-mass end; for simpli-

TABLE 2

CLOSED BOX MODELS[a]

m_{CO}	m_{bh}	r	He	10^3C	10^3Z	$\frac{O}{Z}$	$\frac{Z-C-O}{O}$	$\frac{\Delta Y}{\Delta O}$	$\frac{C}{O}$
60......	No BH	3.39	0.2376	0.619	5.00	0.516	0.700	2.946	0.240
40......	88.2–106	3.05	0.2385	0.686	5.28	0.489	0.780	3.292	0.266
25......	60.4–74.8	2.47	0.2406	0.848	5.96	0.433	0.983	4.108	0.329
15......	42.0–52.8	1.84	0.2444	1.147	7.28	0.354	1.377	5.581	0.445
10......	31.6–41.8	1.38	0.2497	1.578	9.12	0.283	1.924	7.636	0.612
7......	25.1–24.8	0.92	0.2623	2.744	13.4	0.193	3.111	12.52	1.064
5......	20.1–20.1	0.69	0.2774	4.572	17.8	0.144	4.146	18.37	1.772
60......	No BH	5.29	0.2348	0.379	3.17	0.510	0.725	2.970	0.234

[a] For $O = 2.580 \times 10^{-3}$, with the exception of the last model which is for $O = 1.616 \times 10^{-3}$.

TABLE 3

ISM ABUNDANCES BUDGET FOR CLOSED MODELS[a]

t_g (Gyr) (1)	i (2)	SF (3)	LMS (4)	HMS_W (5)	HMS_{SN} (6)	X_i (7)
0.10......	He	-5.623×10^{-1}	3.728×10^{-3}	1.395×10^{-3}	1.638×10^{-2}	2.346×10^{-1}
	C	-2.804×10^{-4}	8.323×10^{-6}	8.607×10^{-6}	6.127×10^{-4}	3.492×10^{-4}
	O	-2.323×10^{-3}	3.819×10^{-6}	6.091×10^{-6}	4.893×10^{-3}	2.580×10^{-3}
	Z	-3.835×10^{-3}	2.331×10^{-4}	2.062×10^{-4}	7.877×10^{-3}	4.481×10^{-3}
1.00......	He	-5.797×10^{-1}	2.148×10^{-2}	1.650×10^{-3}	1.794×10^{-2}	2.367×10^{-1}
	C	-4.807×10^{-4}	3.822×10^{-4}	1.544×10^{-5}	6.629×10^{-4}	5.798×10^{-4}
	O	-2.583×10^{-3}	6.550×10^{-5}	8.859×10^{-6}	5.089×10^{-3}	2.580×10^{-3}
	Z	-4.867×10^{-3}	1.348×10^{-3}	2.991×10^{-4}	8.192×10^{-3}	4.972×10^{-3}
10.0.......	He	-6.003×10^{-1}	4.289×10^{-2}	1.704×10^{-3}	1.810×10^{-2}	2.376×10^{-1}
	C	-6.159×10^{-4}	5.473×10^{-4}	1.688×10^{-5}	6.702×10^{-4}	6.185×10^{-4}
	O	-2.693×10^{-3}	1.502×10^{-4}	9.339×10^{-6}	5.114×10^{-3}	2.580×10^{-3}
	Z	-5.256×10^{-3}	1.725×10^{-3}	3.191×10^{-4}	8.217×10^{-3}	5.004×10^{-3}
10.0.......	He	-5.793×10^{-1}	2.654×10^{-2}	8.107×10^{-4}	1.142×10^{-2}	2.348×10^{-1}
	C	-3.690×10^{-4}	3.311×10^{-4}	2.622×10^{-6}	4.145×10^{-4}	3.792×10^{-4}
	O	-1.625×10^{-3}	6.051×10^{-5}	2.254×10^{-6}	3.178×10^{-3}	1.616×10^{-3}
	Z	-3.194×10^{-3}	1.006×10^{-3}	8.889×10^{-5}	5.266×10^{-3}	3.167×10^{-3}

[a] Adjusting O $= 2.580 \times 10^{-3}$, with the exception of the last model which adjusts O $= 1.616 \times 10^{-3}$.

city, we will assume that it is the slope of the IMF which varies in the $0.01 < m < 0.5$ range. In this case r can be computed as follows:

$$r = \frac{\int_{m_l}^{120} m\xi(m)dm}{\int_{m_l}^{120} m\xi'(m)dm}, \tag{4.1}$$

where m_l is any value greater than 0.5, $\xi(m)$ is the KTG IMF, and $\xi'(m)$ is a slope-modified IMF; both IMFs are normalized to 1. Our results produce a slope for $\xi'(m)$ in the $0.01 < m < 0.5$ interval, whose absolute value increases with r: for the $r > 1$ values shown in the first five rows of Table 2 we obtained, for a decreasing r, the following values for the slope: -2.38, -2.32, -2.21, -2.01, and -1.76. For the model with the S IMF and $m_{CO} = 60$, an r value of 3.20 is obtained, very similar to the r value derived with the KTG IMF. The value 0.5 for m_l comes from one of the points where the KTG IMF changes its slope; however, this point may be moved up to 1 (adjusting the slope correspondingly) without any change in the predicted abundance ratios.

The change in O from 2.58×10^{-3} to 1.62×10^{-3} does not affect significantly the O/Z, $(Z - C - O)/O$, $\Delta Y/\Delta O$, and C/O ratios, the largest change is for the $(Z - C - O)/O$ ratio and amounts to 3.6%. Thus, if an observational error in the determination of O exists and is of the order of a factor of 2, then the conclusions derived from the abundance ratios will still be valid. In addition, the change in the r parameter is inversely proportional to the change in the O abundance.

Similarly, an analysis of the influence of the μ parameter on the predictions by the models, shows that an increase in μ of 10% produces a decrease in r of 7.32%, and a decrease in μ of 10% produces an increase in r of 7.96%. Furthermore, the changes in O/Z, $(Z - C - O)/O$, $\Delta Y/\Delta O$, and C/O are smaller than 0.5%; these models keep M_T constant and vary M_{gas}.

5. OUTFLOW MODELS

5.1. *Outflow of Well-mixed Material*

The adopted $\log \mu$ and O values can also be fitted by assuming that galaxies are ejecting well-mixed material to the intergalactic medium via an ordinary galactic wind. In chemical evolution models with the IRA assumption, an ordinary wind is introduced by assuming an outflow modeled by $f_O = \lambda(1 - R)\psi$, where R is the mass fraction returned to the interstellar medium by a generation of stars. In our models, this wind is introduced as an outflow given by $f_O = \alpha M_{gas}$, where the α parameter is then related to λ through $\alpha = \lambda(1 - R)\nu$. Notice that R is ill defined in the models that do not assume the IRA; nevertheless, an average R value has been defined and used to compute the λ parameter. Models with an outflow of well-mixed material, a KTG IMF, no black holes, and $r = 1$, are shown in Table 4. The first column shows the different ages of the model; the second contains the ratio of the ejected mass, M_{gas}^e, to the total mass; the third and fourth show the values of the α and λ parameters; the fifth shows the mass fraction that remains trapped in stars, $(1 - R)$; and the last four columns show the O/Z, $(Z - C - O)/O$, $\Delta Y/\Delta O$, and C/O values, respectively.

TABLE 4

OUTFLOW OF WELL-MIXED MATERIAL[a]

t_g (Gyr)	$\frac{M_{gas}^e}{M_T}$	α (Gyr^{-1})	λ	$(1 - R)$	$\frac{O}{Z}$	$\frac{Z - C - O}{O}$	$\frac{\Delta Y}{\Delta O}$	$\frac{C}{O}$
0.10......	6.43	29.40	10.77	0.798	0.505	0.821	2.861	0.159
1.00......	6.50	2.932	10.13	0.742	0.486	0.746	3.290	0.312
10.0.......	7.95	0.316	13.13	0.606	0.512	0.703	3.347	0.250
10.0.......	16.07	0.390	27.24	0.587	0.506	0.729	3.530	0.247

[a] O $= 2.580 \times 10^{-3}$ with the exception of the last model which is for O $= 1.616 \times 10^{-3}$.

The $\Delta Y/\Delta O$ values of the models in Table 4 are larger than those predicted by closed box models due to the delay of the He production relative to that of O; this delay causes a preferential O loss to the intergalactic medium.

The increase in the $\Delta Y/\Delta O$ ratios produced by outflow of well-mixed material relative to those produced by closed box models goes in the right direction but is not large enough to explain the observational constraint; this is one of the reasons that has led to the idea of a different type of galactic outflow.

5.2. *Outflow of O-rich Material*

It has been proposed that an outflow of O-rich material is present, at least in some galaxies, to explain (*a*) the small yield in heavy elements seen in irregular galaxies (Lequeux 1989; Tosi 1994; Peimbert et al. 1994a), (*b*) the large helium abundances derived in some irregular and blue compact galaxies (Aparicio, García-Pelayo, & Moles 1988), (*c*) the large $\Delta Y/\Delta O$ ratios derived from samples of galaxies (Aparicio et al. 1988; Lequeux 1989; Pilyugin 1993; Tosi 1994; Peimbert et al. 1994a; Marconi, Matteucci, & Tosi 1994), (*d*) the high Fe/O ratio in the Magellanic Clouds (Russell, Bessell, & Dopita 1988a, b; Lequeux 1989), and (*e*) the *Z*-mass relation present in irregular galaxies (De Young & Gallagher 1990).

By assuming that a fraction γ of the mass of a SN is ejected to the intergalactic medium without mixing with the interstellar gas, several models with a KTG IMF for different values of the parameter γ have been calculated in order to fit the adopted log μ and O values, these models are shown in Tables 5 and 6 and Figures 4, 5, and 6, where the curves are nonlinear fits to the computed models (*solid squares*). The inclusion of SN I's in these models produces a situation analogous to the one produced for the closed models and the resulting predictions are similar to the ones indicated by a dot in Figures 1, 2, and 3.

For a galactic age of 1 Gyr, about half of the freshly made He is ejected by stars in the 7.5–120 $M_\odot$ range and the other half, by stars in the 1.85–7.5 $M_\odot$ range, whereas almost all of the O is produced by high-mass stars; meanwhile, for a galactic age of 10 Gyr, stars in the 0.9–7.5 $M_\odot$ range produce about twice the He produced by high-mass stars. Low-mass stars end their lives as white dwarfs and eject part of their masses in normal stellar winds during the red giant phase and as superwinds during the preplanetary nebula phase; on the other hand, stars in the 7.5–120 $M_\odot$ range lose part of their masses via stellar winds and afterward explode like SN II's; these ejecta have typical initial velocities of a few thousand km s^{-1}, and so a fraction of the ejected mass might be expected to leave the parental galaxy.

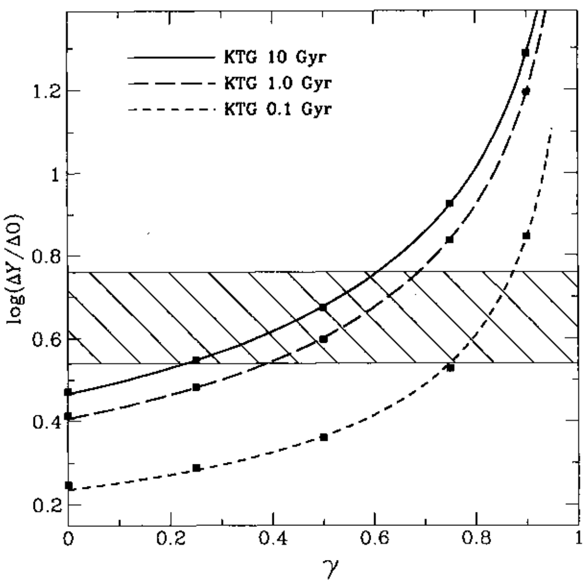

FIG. 4.—$\Delta Y/\Delta O$ vs. γ assuming three different galactic ages. The models (*solid squares*) are adjusted by nonlinear fits given by $a + b/[(1-\gamma)+c]$ (*solid lines*). The shaded band indicates the region allowed by observations.

TABLE 5

OUTFLOW OF O-RICH MATERIAL[a]

t_g (Gyr)	γ	r	$\frac{O}{Z}$	$\frac{\Delta Y}{\Delta O}$	$\frac{Z-C-O}{O}$	$\frac{C}{O}$	$\frac{M^e_{gas}}{M_T}$ (10^{-2})
0.10......	0.00	3.240	0.576	1.783	0.601	0.135	0.190
	0.25	2.442	0.562	1.938	0.642	0.137	1.366
	0.50	1.644	0.536	2.287	0.723	0.141	2.276
	0.75	0.847	0.467	3.372	0.988	0.155	5.159
	0.90	0.370	0.315	7.016	1.939	0.231	14.34
1.00......	0.00	3.290	0.519	2.597	0.702	0.225	0.910
	0.25	2.497	0.489	3.023	0.787	0.257	1.442
	0.50	1.704	0.437	3.953	0.963	0.325	2.428
	0.75	0.910	0.321	6.860	1.566	0.553	5.539
	0.90	0.453	0.165	15.659	3.470	1.604	14.72
10.0	0.00	3.390	0.516	2.946	0.700	0.240	0.910
	0.25	2.599	0.485	3.527	0.784	0.277	1.442
	0.50	1.807	0.431	4.729	0.966	0.356	2.656
	0.75	1.013	0.331	8.411	1.593	0.622	5.615
	0.90	0.562	0.157	19.380	3.519	1.853	14.64
10.0	0.00	5.291	0.510	2.970	0.725	0.235	0.910
	0.25	4.026	0.484	3.527	0.798	0.270	1.214
	0.50	2.760	0.437	4.641	0.948	0.341	1.897
	0.75	1.495	0.331	8.045	1.456	0.561	3.794
	0.90	0.744	0.175	18.750	3.376	1.351	9.712

[a] For O $= 2.580 \times 10^{-3}$ with the exception of the last five models which are for O $= 1.616 \times 10^{-3}$.

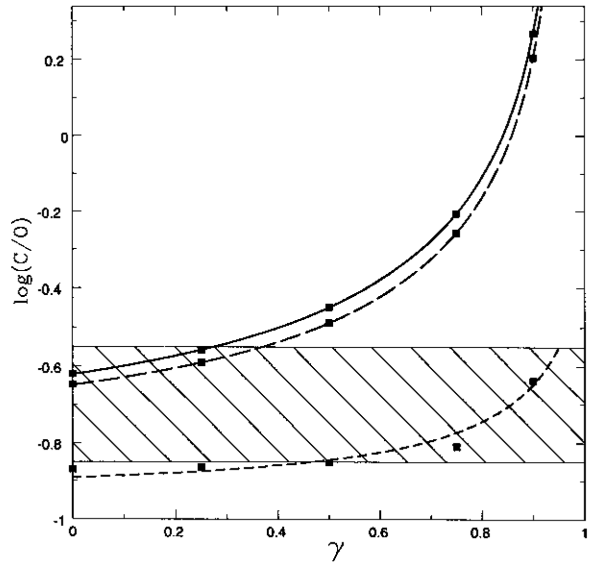

FIG. 5.—Analog of Fig. 4 for C/O

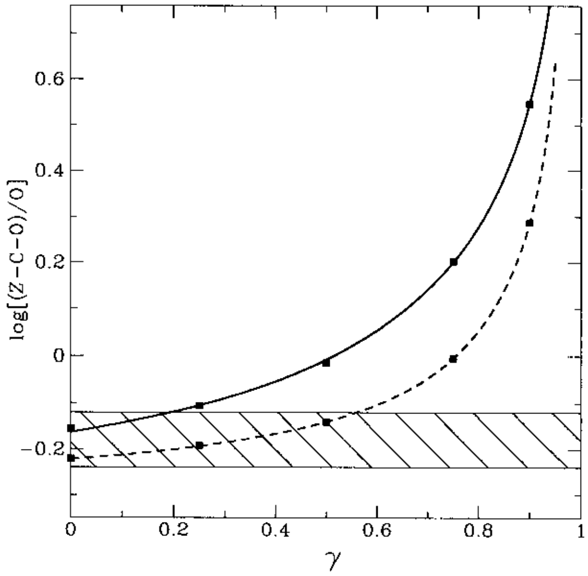

FIG. 6.—Analog of Fig. 4 for $(Z - C - O)/O$. The 1 and 10 Gyr models are almost identical in this case; consequently, only the 10 Gyr model is presented.

TABLE 6

ISM ABUNDANCES BUDGET: MODELS WITH AN OUTFLOW OF O-RICH MATERIAL

t_g (Gyr)	γ	i	SF	GW	LMS	HMS_W	HMS_{SN}	X_i
0.10......	0.25	He	-5.670×10^{-1}	-5.466×10^{-3}	4.992×10^{-3}	1.876×10^{-3}	2.190×10^{-2}	2.350×10^{-1}
		C	-2.839×10^{-4}	-2.048×10^{-4}	1.114×10^{-5}	1.195×10^{-5}	8.195×10^{-4}	3.538×10^{-4}
		O	-2.342×10^{-3}	-1.636×10^{-3}	5.118×10^{-6}	8.281×10^{-6}	6.544×10^{-3}	2.580×10^{-3}
		Z	-3.901×10^{-3}	-2.632×10^{-3}	3.121×10^{-4}	2.798×10^{-4}	1.053×10^{-2}	4.589×10^{-3}
	0.50	He	-5.767×10^{-1}	-1.650×10^{-2}	7.555×10^{-3}	2.861×10^{-3}	3.307×10^{-2}	2.359×10^{-1}
		C	-2.911×10^{-4}	-6.184×10^{-4}	1.686×10^{-5}	1.942×10^{-5}	1.237×10^{-3}	3.638×10^{-4}
		O	-2.381×10^{-3}	-4.940×10^{-3}	7.760×10^{-6}	1.293×10^{-5}	9.880×10^{-3}	2.580×10^{-3}
		Z	-4.038×10^{-3}	-7.940×10^{-3}	4.724×10^{-4}	4.349×10^{-4}	1.588×10^{-2}	4.810×10^{-3}
	0.75	He	-6.075×10^{-1}	-5.052×10^{-2}	1.554×10^{-2}	6.024×10^{-3}	6.749×10^{-2}	2.387×10^{-1}
		C	-3.155×10^{-4}	-1.893×10^{-3}	3.467×10^{-5}	4.949×10^{-5}	2.525×10^{-3}	4.002×10^{-4}
		O	-2.506×10^{-3}	-1.512×10^{-2}	1.605×10^{-5}	2.937×10^{-5}	2.016×10^{-2}	2.580×10^{-3}
		Z	-4.490×10^{-3}	-2.423×10^{-2}	9.719×10^{-4}	9.676×10^{-4}	3.231×10^{-2}	5.530×10^{-3}
10.0.......	0.25	He	-6.181×10^{-1}	-6.035×10^{-3}	5.759×10^{-2}	2.368×10^{-3}	2.422×10^{-2}	2.391×10^{-1}
		C	-7.262×10^{-4}	-2.250×10^{-4}	7.403×10^{-4}	2.652×10^{-5}	9.001×10^{-4}	7.158×10^{-4}
		O	-2.771×10^{-3}	-1.712×10^{-3}	2.013×10^{-4}	1.363×10^{-5}	6.847×10^{-3}	2.580×10^{-3}
		Z	-5.695×10^{-3}	-2.739×10^{-3}	2.331×10^{-3}	4.631×10^{-4}	1.096×10^{-2}	5.318×10^{-3}
	0.50	He	-6.564×10^{-1}	-1.829×10^{-2}	8.791×10^{-2}	3.871×10^{-3}	3.669×10^{-2}	2.422×10^{-1}
		C	-9.699×10^{-4}	-6.867×10^{-4}	1.147×10^{-3}	5.444×10^{-5}	1.374×10^{-3}	9.187×10^{-4}
		O	-2.943×10^{-3}	-5.193×10^{-3}	3.063×10^{-4}	2.470×10^{-5}	1.039×10^{-2}	2.580×10^{-3}
		Z	-6.679×10^{-3}	-8.245×10^{-3}	3.605×10^{-3}	8.172×10^{-4}	1.649×10^{-2}	5.991×10^{-3}
	0.75	He	-7.718×10^{-1}	-5.609×10^{-2}	1.841×10^{-1}	9.868×10^{-3}	7.502×10^{-2}	2.517×10^{-1}
		C	-1.874×10^{-3}	-2.154×10^{-3}	2.517×10^{-3}	2.426×10^{-4}	2.873×10^{-3}	1.604×10^{-3}
		O	-3.458×10^{-3}	-1.595×10^{-2}	6.321×10^{-4}	8.602×10^{-5}	2.127×10^{-2}	2.580×10^{-3}
		Z	-1.028×10^{-2}	-2.476×10^{-2}	7.874×10^{-3}	2.447×10^{-3}	3.301×10^{-2}	8.294×10^{-3}
10.0.......	0.25	He	-5.903×10^{-1}	-3.805×10^{-3}	3.553×10^{-2}	1.112×10^{-3}	1.527×10^{-2}	2.357×10^{-1}
		C	-4.295×10^{-4}	-1.387×10^{-4}	4.452×10^{-4}	4.184×10^{-6}	5.550×10^{-4}	4.362×10^{-4}
		O	-1.655×10^{-3}	-1.062×10^{-3}	8.102×10^{-5}	3.208×10^{-6}	4.249×10^{-3}	1.616×10^{-3}
		Z	-3.411×10^{-3}	-1.756×10^{-3}	1.353×10^{-3}	1.309×10^{-4}	7.023×10^{-3}	3.341×10^{-3}
	0.50	He	-6.121×10^{-1}	-1.146×10^{-2}	5.371×10^{-2}	1.765×10^{-3}	2.300×10^{-2}	2.375×10^{-1}
		C	-5.566×10^{-4}	-4.197×10^{-4}	6.790×10^{-4}	8.682×10^{-6}	8.397×10^{-4}	5.510×10^{-4}
		O	-1.715×10^{-3}	-3.203×10^{-3}	1.226×10^{-4}	5.508×10^{-6}	6.406×10^{-3}	1.616×10^{-3}
		Z	-3.868×10^{-3}	-5.269×10^{-3}	2.063×10^{-3}	2.351×10^{-4}	1.054×10^{-2}	3.699×10^{-3}
	0.75	He	-6.801×10^{-1}	-3.479×10^{-2}	1.100×10^{-1}	4.171×10^{-3}	4.653×10^{-2}	2.430×10^{-1}
		C	-9.903×10^{-4}	-1.291×10^{-3}	1.428×10^{-3}	3.823×10^{-5}	1.722×10^{-3}	9.068×10^{-4}
		O	-1.901×10^{-3}	-9.748×10^{-3}	2.505×10^{-4}	1.675×10^{-5}	1.300×10^{-2}	1.616×10^{-3}
		Z	-5.453×10^{-3}	-1.580×10^{-2}	4.335×10^{-3}	7.251×10^{-4}	2.106×10^{-2}	4.876×10^{-3}

The first column of Table 5 shows the galactic age; the chosen gamma values and the corresponding r values are shown in the second and third columns, respectively; the fourth, fifth, sixth, and seventh columns show the computed values of O/Z, $\Delta Y/\Delta O$, $(Z - C - O)/O$, and C/O, respectively; finally, the last column shows the ratio of the ejected mass, M_{gas}^e, to the total mass. As one would expect, the $\Delta Y/\Delta O$ value increases if the γ value increases. The gamma value with $r = 1$ means that the corresponding O-rich wind is sufficient to reproduce the adopted log μ and O values; i.e., there is no need for a modified IMF at the low-mass end. A value of r smaller than 1 indicates that the fraction of stars at the low-mass end of the IMF is smaller than that given by the KTG IMF.

As can be seen from Figures 4 and 5, for a given IMF, the dependence of $\Delta Y/\Delta O$ and C/O with t_g is like the one reported above for the γ-dependence of $\Delta Y/\Delta O$: if t_g increases, more C and He produced by the LMS will be ejected to the ISM and so the $\Delta Y/\Delta O$ and C/O values increase; this behavior is not followed by $(Z - C - O)/O$ when going from 1 to 10 Gyr (Fig. 6) since most of the $(Z - C - O)$ elements are ejected by stars with $m_i > 1.85$. If γ increases, then r decreases and the number of stars that participate in the enrichment of the ISM increases; therefore, the production rate of any element increases. The nonlinear fits to the models in Figures 4, 5, and 6 were obtained assuming that the logarithm of the ratio of any element to O varies as $a + b/[(1 - \gamma) + c]$, where a, b, and c are numbers to be determined for each element.

It follows from Figures 4, 5, and 6 that there is not a unique γ value that fits the three observational constraints at a given age. As in the case of the closed box models, two possibilities can be followed: (*a*) to adopt models that fit the $\Delta Y/\Delta O$ but not the C/O and $(Z - C - O)/O$ constraints (those with high γ and low r values, e.g., $\gamma = 0.6$ and $r = 1.4$ for a $t_g = 10$ Gyr); or (*b*) to adopt the models that reproduce the C/O and $(Z - C - O)/O$ but not the $\Delta Y/\Delta O$ constraints (those with low γ and high r values, e.g., $\gamma = 0$ and $r = 3.39$ for the same $t_g = 10$ Gyr). It should be mentioned, however, that there is a model ($\gamma \sim 0.23$ and an $r \sim 2.66$ for a $t_g = 10$ Gyr) which barely fits the three observational constraints; note that this model requires a slope of -2.25 for the IMF in the $0.01 < m_i < 0.5$ interval, a value which is steeper than -1.3, the slope of the IMF for the solar vicinity in the same interval. This result for metal-poor galaxies supports the idea that the fraction of small-mass stars does decrease with increasing metallicity (Peimbert & Serrano 1982; Gusten & Mezger 1983; Larson 1986; Richer et al. 1991).

Table 6 is analogous to Table 3, but including two additional columns: the second and the fifth, that show the γ values and the galactic wind contributions by gas mass, respectively.

6. CONCLUSIONS

We present chemical evolution models for irregular galaxies in order to try to fit five observational constraints. We study the parameter space provided by (*a*) t_g, i.e., without IRA; (*b*) closed box models varying m_{CO}; for each m_{CO} a different r is needed to match log μ and O; (*c*) well-mixed outflow models with $r = 1$; and (*d*) O-rich outflow models varying γ; for each γ a different r is needed to match log μ and O.

As various authors have previously pointed out, closed models with a solar vicinity IMF do not explain the low O abundances.

The low O abundances require a change in the IMF: either a larger amount of low-mass stars or a change in the slope at the high-mass end. We present arguments against a change in the slope of the IMF at the high-mass end and conclude that the change should be at the low-mass end according to the r parameter defined by equation (4.1).

The production of black holes that prevent stars with masses higher than m_{bh} from enriching the ISM can explain μ, O, and $\Delta Y/\Delta O$ with an $r = 1.97$ and $m_{CO} = 16.4$. This model fails to explain the C/O and $(Z - C - O)/O$ observational constraints. We consider that black holes do not play an important role in the chemical evolution of irregular galaxies due to their failure at explaining C/O and $(Z - C - O)/O$ and also due to the results of chemical evolution models for the solar neighborhood that do not require them.

The best closed models are those without black holes, and among them, the one with $t_g = 10$ Gyr, a KTG IMF, and $r = 3.39$ is best since (*a*) there is evidence of star formation during about 10 Gyr in Magellanic irregulars; (*b*) it explains μ, O, C/O, and $(Z - C - O)/O$; and (*c*) it is the model that comes closer to explaining the $\Delta Y/\Delta O$ constraint.

Errors or changes in O and μ of a factor of 2 or less produce changes smaller than 4% in the model-predicted $\Delta Y/\Delta O$, C/O, and $(Z - C - O)/O$ values. Alternatively, the changes in r are larger and are (*a*) inversely proportional to the changes in O and (*b*) proportional to changes in log (μ^{-1}).

Our models have been obtained trying to fit the observational constraints of a "typical" irregular galaxy, defined as the average of the properties of the 10 selected galaxies in Table 1. Nevertheless, our models are robust and can be generalized to individual galaxies with changes of about a factor of 2 in O and a factor of 2 in μ, relative to our "typical" irregular. This range of values includes most of the galaxies in Table 1 with the exception of the two metal poorest that might need a different set of chemical evolution models and that were mainly used to determine Y_p.

We computed outflow models with well-mixed material and $r = 1$ that fitted μ, O, C/O, and $(Z - C - O)/O$. These models predict $\Delta Y/\Delta O$ values closer to the observed ones but not close enough; they also predict large M_{gas}^e/M_T values; the ejected gas, however, has probably dissipated for a $t_g = 10$ Gyr model and would be difficult to detect. Well-mixed outflow models made to fit μ and O with r values between 1 and those of the closed models would yield $\Delta Y/\Delta O$, C/O, and $(Z - C - O)/O$ values intermediate between those presented in Table 4 and the closed box models.

Outflow models of O-rich material with $\gamma = 0.23$ and $r = 2.66$ can marginally fit μ, O, $\Delta Y/\Delta O$, C/O, and $(Z - C - O)/O$. Lower values of γ (requiring $r > 2.66$ values) fail to fit $\Delta Y/\Delta O$; while larger values of γ (requiring $r < 2.66$ values) fail to fit C/O and $(Z - C - O)/O$. A better agreement with the three abundance ratios could be obtained for a smaller observed value of $\Delta Y/\Delta O$, and this could be so if the effect on the O abundance due to the temperature structure of the H II regions is higher than the one adopted in this study.

The best fit to the five observational constraints is given by O-rich outflows with $\gamma = 0.23$ and $r = 2.66$. For this model we obtain a slope of -2.25 for the low-mass end of the IMF; this slope is intermediate between the KTG IMF slope of -1.3 and a slope smaller than -2.5 derived by Richer et al. (1991) for globular clusters. The metallicity of our "typical" irregular galaxy is intermediate between that of the solar vicinity and those of the globular clusters; the change in the slope could therefore be due to a metallicity effect.

The authors express their gratitude to D. R. Garnett for reading the manuscript and for his excellent suggestions, and to J. S. Mathis for fruitful discussions. They also acknowledge a thorough arbitration by B. E. J. Pagel, whose criticism and comments helped to improve and clarify the manuscript.

REFERENCES

Aparicio, A., García-Pelayo, J. M., & Moles, M. 1988, A&AS, 74, 375
Biémont, E., Baudoux, M., Kurucz, R. L., Ansbacher, W., & Pinnington, E. H. 1991, A&A, 249, 539
Campbell, A. 1988, ApJ, 335, 644
Carigi, L. 1994, ApJ, 424, 181
De Young, D. S., & Gallagher, J. S. 1990, ApJ, 356, L15
Draine, B. T., & Lee, H. M. 1984, ApJ, 285, 89
Dufour, R. J., Shields, G. A., & Talbot, R. J. 1981, ApJ, 252, 461
Dufour, R. J., et al. 1995, in preparation
Garnett, D. R. 1990, ApJ, 363, 142
Garnett, D. R., Skillman, E. D., Dufour, R. J., Peimbert, M., Torres-Peimbert, S., Terlevich, R. J., Terlevich, E., & Shields, G. A. 1995, ApJ, 443, 64
González-Delgado, R. M., et al. 1994, ApJ, 437, 239
Grevesse, N., & Anders, E. 1989, in Cosmic Abundances of Matter, ed. J. Waddington (New York: American Institute of Physics), 1
Grevesse, N., Lambert, D. L., Sauval, A. J., van Dishoeck, E. F., Farmer, C. B., & Norton, R. H. 1990, A&A, 232, 225
Gusten, R., & Mezger, P. G. 1983, Vistas Astr., 26, 159
Hannaford, P., Lowe, R. M., Grevesse, N., & Noels, A. 1992, A&A, 259, 301
Holweger, H., Bard, A., Kock, A., & Kock, M. 1991, A&A, 249, 545
Izotov, Y. I., Thuan, T. X., & Lipovetsky, V. A. 1994, ApJ, 435, 647
Kroupa, P., Tout, C. A., & Gilmore, G. 1993, MNRAS, 262, 545 (KTG)
Kunth, K. D., & Sargent, W. L. W. 1983, ApJ, 273, 81
Larson, R. B. 1986, MNRAS, 218, 409
Lequeux, J. 1989, in Evolution of Galaxies—Astronomical Observations, ed. I. Appenzeller, H. J. Habing, & P. Lena (Berlin: Springer), 147
Lequeux, J., Peimbert, M., Rayo, J., Serrano, A., & Torres-Peimbert, S. 1979, A&A, 80, 155
Maeder, A. 1991, Pré-Publications de L'Observatoire de Genève, Série C, 84
———. 1992, A&A, 264, 105
———. 1993, A&A, 268, 833
Marconi, G., Matteucci, F., & Tosi, M. 1994, MNRAS, 270, 35
Massey, P., Garmany, C. D., Silkey, M., & DeGioia-Eastwood, D. K. 1989a, AJ, 97, 107
Massey, P., Parker, J. W., & Garmany, C. D. 1989b, AJ, 98, 1305
Mathis, J. S. 1994, ApJ, 422, 176
Mathis, J. S., Rumpl, W., & Nordsieck, K. H. 1977, ApJ, 217, 425
McGaugh, S. S. 1991, ApJ, 380, 140
Nomoto, K., Shigeyama, T., & Tsujimoto, T. 1990, in IAU Symp. 145, Evolution of Stars: The Photospheric Abundance Connection, ed. G. Michaud & A. Tutukov (Dordrecht: Kluwer), 21
Pagel, B. E. J. 1987, in A Unified View of the Macro- and the Micro-cosmos, ed. A. de Rújula, D. V. Nanopoulos, & P. A. Shaver (Singapore: World Scientific), 399
Pagel, B. E. J., Simonson, E. A., Terlevich, R. J., & Edmunds, M. G. 1992, MNRAS, 255, 325 (PSTE)
Parker, J. W., & Garmany, C. D. 1993, AJ, 106, 1471
Parker, J. W., Garmany, C. D., Massey, P., & Walborn, N. R. 1992, AJ, 103, 1205
Peimbert, M. 1993, Rev. Mexicana Astron. Af., 27, 9
Peimbert, M., Colín, P., & Sarmiento, A. 1994a, in Violent Star Formation from 30 Doradus to QSOs, ed. G. Tenorio-Tagle (Cambridge: Cambridge Univ. Press), 79
Peimbert, M., Peña, M., & Torres-Peimbert, S. 1986, A&A, 158, 266
Peimbert, M., Sarmiento, A., & Colín, P. 1994b, Rev. Mexicana Astron. Af., 28, 181
Peimbert, M., Sarmiento, A., & Fierro, J. 1991, PASP, 103, 815
Peimbert, M., & Serrano, A. 1982, MNRAS, 198, 563
Peimbert, M., Storey, P. J., & Torres-Peimbert, S. 1993a, ApJ, 414, 626
Peimbert, M., & Torres-Peimbert, S. 1976, ApJ, 203, 581
Peimbert, M., Torres-Peimbert, S., & Dufour, R. J. 1993b, ApJ, 418, 760
Peimbert, M., Torres-Peimbert, S., & Ruiz, M. T. 1992, Rev. Mexicana Astron. Af., 24, 155
Pilyugin, L. S. 1993, A&A, 277, 42
Prantzos, N., Vangioni-Flam, E., & Chauveau, S. 1994, A&A, 285, 132
Renzini, A., & Voli, M. 1981, A&A, 94, 175
Richer, H. B., Fahlman, G. G., Buonanno, R., Fusi Pecci, F., Searle, L., & Thompson, I. B. 1991, ApJ, 381, 147
Rosa, M. R., & Benvenuti, P. 1994, A&A, 291, 1
Russell, S. C., Bessell, M. S., & Dopita, M. A. 1988a, in Galactic and Extragalactic Star Formation, ed. R. E. Pudritz & M. Fich (Dordrecht: Kluwer), 106
———. 1988b, in The Impact of Very High S/N Spectroscopy, ed. G. Cayrel de Strobel & M. Spite (Dordrecht: Kluwer), 545
Salpeter, E. E. 1955, ApJ, 121, 161 (S)
Scalo, J. M. 1986, Fund. Cosmic Phys., 11, 1
Schaller, G., Schaerer, D., Meynet, G., & Maeder, A. 1992, A&ASS, 96, 269
Schmidt, K. H., & Boller, T. 1993, Astron. Nachr., 314, 361
Skillman, E. D. 1991, PASP, 103, 919
Skillman, E. D., & Kennicutt, R. C. 1993, ApJ, 411, 655
Skillman, E. D., Kennicutt, R. C., & Hodge, P. W. 1989, ApJ, 347, 875
Skillman, E. D., Terlevich, R. J., Kennicut, R. C., Garnett, D. R., & Terlevich, E. 1994, ApJ, 431, 172
Staveley-Smith, L., Davies, R. D., & Kinman, T. D. 1992, MNRAS, 258, 334
Torres-Peimbert, S., Peimbert, M., & Fierro, J. 1989, ApJ, 345, 186
Tosi, M. 1994, preprint
Vigroux, L., Stasinska, G., & Comte, G. 1987, A&A, 172, 15